Bachir Bentouati[1], Saliha Chettih[1], Pradeep .Jangir [2], Indrajit N. Trivedi[2]

J. Electrical Systems 12-4 (2016): 716-733

Regular paper

A solution to the optimal power flow using multi-verse optimizer

Journal of Electrical Systems

In this work, the most common problem of the modern power system named optimal power flow (OPF) is optimized using the novel meta-heuristic optimization Multi-verse Optimizer(MVO) algorithm. In order to solve the optimal power flow problem, the IEEE 30-bus and IEEE 57-bus systems are used. MVO is applied to solve the proposed problem. The problems considered in the OPF problem are fuel cost reduction, voltage profile improvement, voltage stability enhancement. The obtained results are compared with recently published meta-heuristics. Simulation results clearly reveal the effectiveness and the rapidity of the proposed algorithm for solving the OPF problem.

Keywords: Optimal power flow; Voltage stability; Power system; Multi-verse Optimizer; Constraints.

Article history: Received 30 March 2016, Accepted 3 November 2016

1. Introduction

At the present time, The optimal power flow (OPF) is a very significant problem and most focused objective for power system planning and operation [1]. The OPF is the elementary tool which permits the utilities to identify the economic operational and many secure states in the system [2], [3]. The OPF problem is one of the utmost operating desires of the electrical power system [4]. The prior function of OPF problem is to evaluate the optimum operational state for bus system by minimizing each objective function within the limits of the operational constraints like equality constraints and inequality constraints [5]. Hence, the OPF problem can be defined as an extremely non-linear and non-convex multimodal optimization problem [6].

From the past few years too many optimization techniques were used for the solution of the OPF problem. Some traditional methods are used to solve the proposed problem have been suffered from some limitations like converging at local optima, not suitable for binary or integer problems and also have the assumptions like the convexity, differentiability, and continuity [7]. Hence, these techniques are not suitable for the actual OPF situation [8], [9]. All these limitations are overcome by meta-heuristic optimization methods like genetic algorithm (GA), particle swarm optimization algorithm (PSO), ant colony algorithm (ACO), differential evolution algorithm (DEA),harmony search algorithm (HSA) and biogeography-based Optimization (BBO) [10], [11] and [12], moth-flame optimizer (MFO) [13].

[*] Corresponding author: B.Bentouati, LACoSERE laboratory, Amar Telidji University, 03000 Laghouat, Algeria-mail: b.bentouati@lagh-univ.dz

[1] LACoSERE laboratory, Amar Telidji University, 03000 Laghouat, Algeria

[2] Department of Electrical Engineering Lukhdhirji Engineering College Morbi-Gujarat, India

In this paper, a newly introduced meta-heuristic optimization technique named Multi-verse Optimizer (MVO) is applied to solve the OPF problem. The MVO technique is a biological and sociological inspired algorithm. This technique is based on three concepts in cosmology: white hole, black hole, and wormhole. The capabilities of MVO are finding the fast convergence rate due to the use of roulette wheel selection, can handle continuous and discrete optimization problems.

In this work, the MVO is applied on IEEE 30-bus and IEEE 57-bus systems [15] to solve the OPF [16-20] problem. There are different objective cases considered in this paper that have to be optimize using Multi-verse Optimizer (MVO) technique are fuel cost reduction, voltage stability improvement, and voltage deviation minimization and others. The result shows the optimal adjustments of control variables in accordance with their limits. The results obtained using MVO technique has been compared with Particle Swarm Optimization (PSO) and Firefly Algorithm (FA) techniques. The results show that MVO gives better optimization values as compared to other methods which prove the effectiveness of the proposed algorithm.

2. Optimal Power Flow Problem Formulation

As specified before, OPF is Optimized power flow problem which provides the optimal values of control (independent) variables by minimizing a predefined objective function with respect to the operating bounds of the system [1]. The OPF problem can be mathematically expressed as a non-linear constrained optimization problem as follows [1]:

Minimize $f(a,b)$ (1)

Subject to $s(a,b)=0$ (2)

And $h(a,b)\leq 0$ (3)

Where, a is vector of state variables, b is vector of control variables, $f(a,b)$ is objective function, $s(a,b)$ is different equality constraints set, $h(a,b)$ different inequality constraints set.

2.1 Variables

2.1.1 Control variables

The control variables should be adjusted to satisfy the power flow equations. For the OPF problem, the set of control variables can be formulated as [1], [5]:

$$b^T = [P_{G_2} \dots P_{G_{NLB}}, V_{G_1} \dots V_{G_{NLB}}, Q_{C_1} \dots Q_{C_{NCom}}, T_1 \dots T_{NTr}] \quad (4)$$

Where, P_G and V_G are the real power output at the *PV (Generator)* buses excluding at the slack and (Reference) bus and magnitude of Voltage at *PV* (*Generator*) buses, respectively. Q_C and T are the shunt *VAR* compensation and tap settings of the transformer.

NLB, NTr, NCom No. of generator units, No. of tap changing transformers and No. of shunt *VAR* compensation devices, respectively.

2.1.2 State variables

There is a need for variables for all OPF formulations for the characterization of the Electrical Power Engineering state of the system. So, the state variables can be formulated as [1], [5]:

$$a^T = [P_{G_1}, V_{L_1} \dots V_{L_{NLB}}, Q_{G_1} \dots Q_{G_{NLB}}, S_{l_1} \dots S_{l_{Nline}}] \quad (5)$$

Where, P_{G_1} and V_L are the real power generation at the slack bus and magnitude of Voltage at *PQ (Load)* buses. V_L is magnitude of Voltage at *PQ (Load)* buses, Q_G is reactive power generation of all generators and S_l represent the transmission line loading or line flow. *NLB*, *Nline* represents the No. of *(PQ)* load buses and the No. of transmission lines, respectively.

2.2 Constraints

There are two OPF constraints named inequality and equality constraints. These constraints are explained in the following sections.

2.2.1 Equality constraints

The physical condition of the power system is described by the equality constraints of the OPF. These equality constraints are basically the power flow equations which can be explained as follows [1], [5].

2.2.1.1 Real power constraints

The real power constraints can be formulated as follows:

$$P_{Gi} - P_{Di} - V_i \sum_{J=i}^{NB} V_j [G_{ij} Cos(\delta_{ij}) + B_{ij} Sin(\delta_{ij})] = 0 \tag{6}$$

2.2.1.2 Reactive power constraints

The reactive power constraints can be formulated as follows:

$$Q_{Gi} - Q_{Di} - V_i \sum_{J=i}^{NB} V_j [G_{ij} Cos(\delta_{ij}) + B_{ij} Sin(\delta_{ij})] = 0 \tag{7}$$

Where, $\delta_{ij} = \delta_i - \delta_j$

Where, *NB* is total No. of buses, P_G and Q_G are active and reactive power output, P_D and Q_D are active and reactive power load demand, B_{ij} and G_{ij} are the elements of the admittance matrix $Y_{ij} = (G_{ij} + jB_{ij})$ shows the susceptance and conductance between bus *i* and bus *j*, respectively.

2.2.2 Inequality constraints

The boundaries of power system devices together with the bounds created to surety system security are given by inequality constraints of the OPF [5], [6].

2.2.2.1 Generator constraints.

For all generating units including the slack bus: voltage, active power, and reactive power outputs should be constrained by their minimum and maximum bounds as follows:

$$V_{G_i}^{lower} \le V_{G_i} \le V_{G_i}^{upper}, \ i=1,\ldots,NLB \tag{8}$$

$$P_{G_i}^{lower} \le P_{G_i} \le P_{G_i}^{upper}, \ i=1,\ldots,NLB \tag{9}$$

$$Q_{G_i}^{lower} \le Q_{G_i} \le Q_{G_i}^{upper}, \ i=1,\ldots, NLB \tag{10}$$

2.2.2.2 Transformer constraints

Transformer tap settings should be constrained inside their stated minimum and maximum bounds as follows:

$$T_{G_i}^{lower} \le T_{G_i} \le T_{G_i}^{upper}, \ i=1,\ldots,NLB \tag{11}$$

2.2.2.3 Shunt VAR compensator constraints

Shunt VAR compensators need to be constrained by their minimum and maximum bounds as follows:

$$Q_{C_i}^{lower} \le Q_{GC_i} \le Q_{C_i}^{upper}, \text{ i=1,…,NLB} \tag{12}$$

2.2.2.4 Security constraints.

These comprise the limits of the magnitude of the voltage at *PQ* buses and transmission line loadings. Voltage for every load (*PQ*) bus should be limited by its minimum and maximum operational bounds. Line flow over each transmission line should not exceed its maximum loading limit. So, these limitations can be mathematically expressed as follows [7]:

$$V_{L_i}^{lower} \le V_{L_i} \le V_{L_i}^{upper}, i=1,\ldots,NLB \tag{13}$$

$$S_{l_i} \le S_{l_i}^{upper}, i=1,\ldots,Nline \tag{14}$$

The control variables are self-constraint. The inequality constrained of state variables comprises a magnitude of load *(PQ)* bus voltage, active power production at reference bus, reactive power production, and line loading may be encompassed by an objective function in terms of quadratic penalty terms. In which, the penalty factor is multiplied by the square of the disregard value of state variables and is included in the objective function and any impractical result achieved is declined [7].

Penalty function can be mathematically formulated as follows:

$$J_{aug} = J + \partial_P \left(P_{G_1} - P_{G_1}^{lim}\right)^2 + \partial_V \sum_{i=1}^{NLB} (V_{L_i} - V_{L_i}^{lim})^2 + \partial_Q \sum_{i=1}^{NGen} + \partial_S \sum_{i=0}^{Nline} (S_{l_i} - S_{l_i}^{max})^2 \tag{15}$$

Where, $\partial_P, \partial_V, \partial_Q, \partial_S =$ penalty factors

U_{lim} is boundary value of the state variable U.

If U is greater than the maximum limit, U_{lim} takings the value of this one, if U is lesser than the minimum limit U_{lim} takings the value of that limit. This can be shown as follows [7]:

$$U^{lim} = \begin{cases} U^{upper} & ; U > U^{upper} \\ U^{lower} & ; U < U^{lower} \end{cases} \tag{16}$$

3.Multi-Verse Optimizer

Three notions such as black hole, white hole and wormhole shown in Figure. 1 are the main motivation of the MVO algorithm. These three notions are formulated in mathematical models to evaluate exploitation, exploration and local search, respectively. The white hole assumed to be the main part to produce universe. Black holes are attracting all due to its tremendous force of gravitation. The wormholes behave as time/space travel channels in which objects can moves rapidly in universe. Main steps uses to the universes of MVO [15]:

a. If the inflation rate is greater, the possibility of presence of white hole is greater.
b. If the inflation rate is greater, the possibility of presence of black hole is lower.
c. Universes having greater inflation rate are send the substances through white holes.
d. Universes having lesser inflation rate are accepting more substances through black holes.

e. The substances/objects in every universe can create random movement in the direction of the fittest universe through worm holes irrespective to the inflation rate. The objects are move from a universe having higher inflation rate to a universe having lesser inflation rate. It can assure the enhancement of the average inflation rates of the entire cosmoses with the iterations. In each iteration, the universes are sorted according to their inflation rates and select one from them using the roulette wheel as a white hole. The subsequent stages are used for this procedure. Assume that

$$U = \begin{bmatrix} x_1^1 & x_1^2 & . & . & x_1^d \\ x_2^1 & x_2^2 & . & . & x_2^d \\ . & . & . & . & . \\ . & . & . & . & . \\ x_n^1 & x_n^2 & . & . & x_n^d \end{bmatrix} \tag{17}$$

Where, d shows the no. of variables and n shows the no. of candidate solutions:

$$x_i^j = \begin{cases} x_k^j \ ; r1 < NI(Ui) \\ x_i^j \ ; r1 \geq NI(Ui) \end{cases} \tag{18}$$

Where, x_i^j shows the j^{th} variable of i^{th} universe, U_i indicates the i^{th} universe, $NI(U_i)$ is normalized inflation rate of the i^{th} universe, $r1$ is a random no. from [0, 1], and x_k^j shows the j^{th} variable of k^{th} universe chosen through a roulette wheel. To deliver variations for all universe and more possibility of increasing the inflation rate by worm holes, suppose that worm hole channels are recognized among a universe and the fittest universe created until now. This mechanism is formulated as:

$$x_i^j = \begin{cases} \begin{cases} X_j + TDR \times ((ub_j - lb_j) \times r4 + lb_j); r3 < 0.5 \\ X_j - TDR \times ((ub_j - lb_j) \times r4 + lb_j); r3 \geq 0.5 \end{cases} ; r2 < WEP \\ x_i^j ; r2 \geq WEP \end{cases} \tag{19}$$

Where X_j shows j^{th} variable of fittest universe created until now, lb_j indicates the min limit of j^{th} parameter, ub_j indicates max limit of j^{th} parameter, x_i^j shows the j^{th} parameter of i^{th} universe, and r2, r3, r4 are random numbers from [0, 1]. It can be concluded by the formulation that wormhole existence probability (*WEP*) and travelling distance rate (*TDR*) are the chief coefficients. The formulation for these coefficients are given by:

$$WEP = \min + l \times \left(\frac{\max - \min}{L} \right) \tag{20}$$

Where, l shows the present run, and L represent maximum run number/iteration, min is the minimum 0.2 in this paper, max is the maximum 1 in this paper.

$$TDR = 1 - \frac{l^{1/p}}{L^{1/p}} \tag{21}$$

Where, p states the accuracy of exploitation with the iterations. If the p is greater, the exploitation is faster and more precise. The complexity of the MVO algorithms based on the no. of iterations, no. of universes, roulette wheel mechanism, and universe arranging mechanism. The overall computational complexity is as follows:

$$O(MVO) = O(l(O(Quicksort) + n \times d \times (O(roulette\_wheel)))) \tag{22}$$

$$O(MVO) = O(l(n^2 + n \times d \times \log n)) \tag{23}$$

Where, n shows no. of universes, l shows the maximum no. of run/iterations, and d shows the no. of substances.

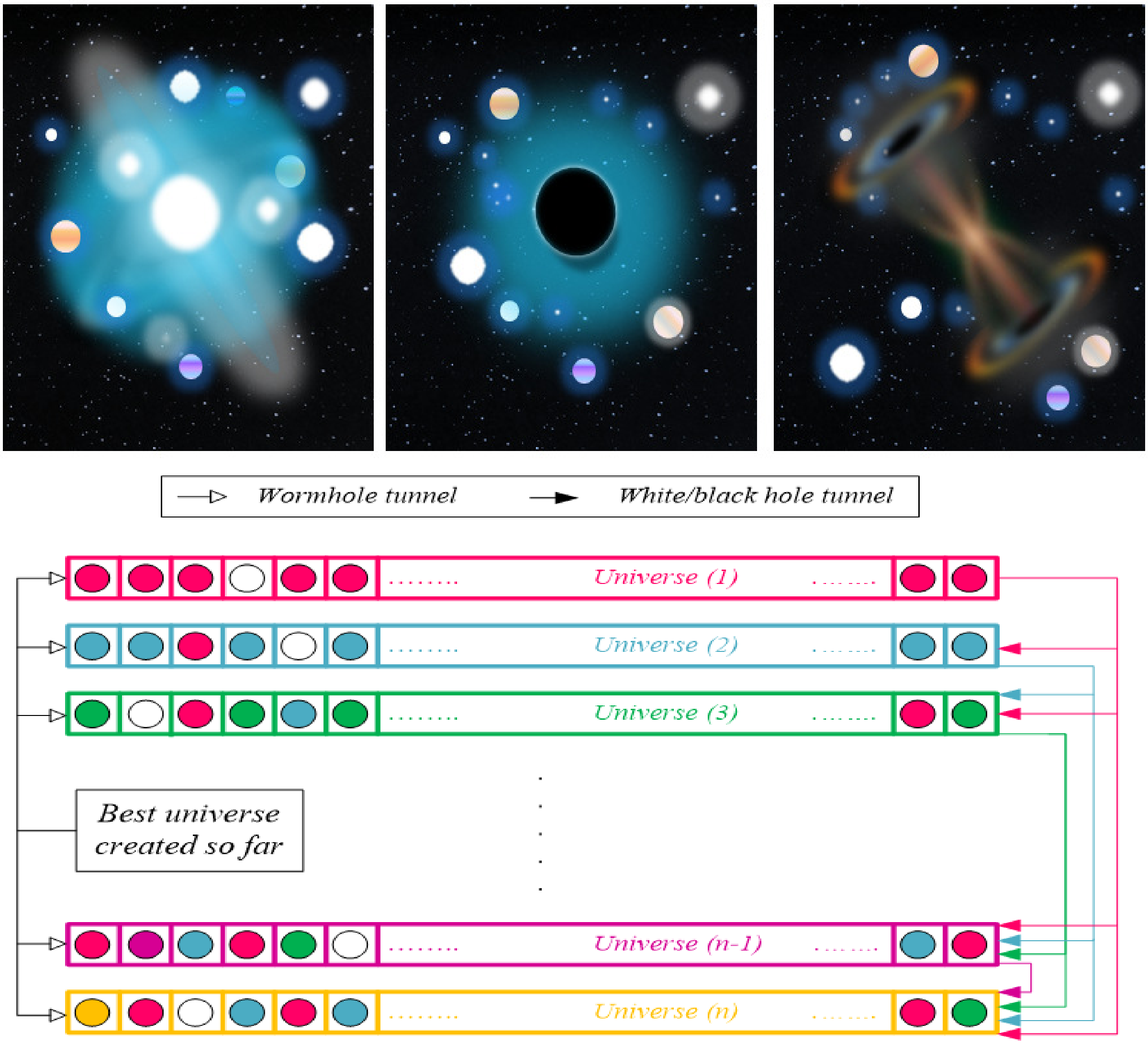

Figure. 1: Basic principle of MVO

4. Application and results

The MVO technique has been implemented for the OPF problem solution for standard IEEE 30-bus and IEEE 57-bus test systems and for a number of cases with dissimilar objective functions. The developed software program is written in MATLAB R2014b computing surroundings and used on a 2.60 GHz i5 PC with 4 GB RAM. In this work, the MVO population size or number of ants is selected to be 40, and the maximum number of iteration is 500.

4.1 IEEE 30-bus test system

With the purpose of elucidating the effectiveness of the suggested MVO algorithm, it has been verified on the standard IEEE 30-bus test system. The standard IEEE 30-bus test system selected in this work has the following characteristics [7], [14]: six generating units at buses 1,2,5,8,11 and 13, four regulating transformers with off-nominal tap ratio between buses 4-12, 6-9, 6-10 and 28-27 and nine shunt VAR compensators at buses 10,12,15,17,20,21,23,24 and 29.

In addition, generator cost coefficient data, the line data, bus data, and the upper and lower bounds for the control variables are specified in [14].

In given test system, five diverse cases have been considered for various purposes and all the acquired outcomes are given in Table 2. The very first column of this table denotes the optimal values of control variables found where:

- P_{G1} through P_{G6} and V_{G1} through V_{G6} signifies the power and voltages of generator 1 to generator 6.
- $T_{4\text{-}12}$, $T_{6\text{-}9}$, $T_{6\text{-}10}$ and $T_{28\text{-}27}$ are the transformer tap settings comprised between buses 4-12, 6-9, 6-10 and 28-27.
- Q_{C10}, Q_{C12}, Q_{C15}, Q_{C17}, Q_{C20}, Q_{C21}, Q_{C23}, Q_{C24} and Q_{C29} denote the shunt VAR compensators coupled at buses 10, 12, 15, 17, 20, 21, 23, 24 and 29.

Further, fuel cost *($/h)*, real power losses *(MW)*, reactive power losses *(MVAR)*, voltage deviation and *Lmax* represent the total generation fuel cost of the system, the total real power losses, the total reactive power losses, the load voltages deviation from 1 and the stability index, respectively. Other particulars for these outcomes will be specified in the next sections.

Case 1: Minimization of generation fuel cost.

The very common OPF objective that is generation fuel cost reduction is considered in the case 1. Therefore, the objective function *Y* represents the total fuel cost of all generating units and it is calculated by following equation [1]:

$$Y = \sum_{i=1}^{NLB} f_i (\$/h) \tag{24}$$

Where, f_i is the fuel cost of the i^{th} *generator*.

f_i, may be formulated as follow:

$$f_i = u_i + v_i P_{Gi} + w_i P_{Gi}^2 (\$/h) \tag{25}$$

Where, u_i, v_i and w_i are the basic, the linear and the quadratic cost coefficients of the i^{th} generator, respectively. The cost coefficients values are specified in [14].

The variation of the total fuel cost over iterations is presented in Figure.2. It demonstrates that the suggested method has outstanding convergence characteristics. The optimal values of control variables obtained for case 1 are specified in Table 1. By means of the same settings i.e. control variables boundaries, initial conditions, and system data, the results achieved in case 1 with the MVO technique are compared to some other methods and it displays that the total fuel cost is greatly reduced compared to the initial case [7]. Quantitatively, it is reduced from 901.951*$/h* to 799.242*$/h*. The comparison of fuel cost obtained with different methods is shown in Table 2 which displays that the results obtained by MVO are better than the other methods.

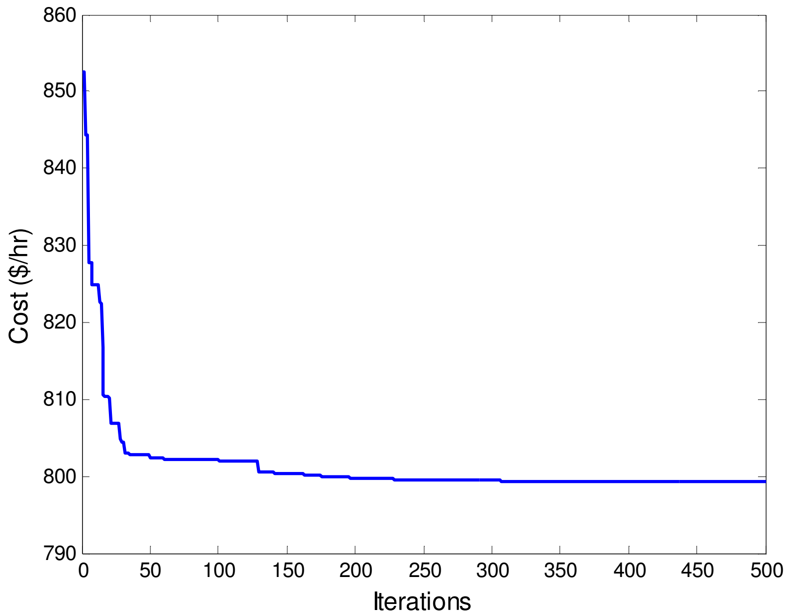

Figure.2 Fuel cost variation for Case 1.

Case 2: Voltage profile improvement.

Bus voltage is considered as most essential and important security and service excellence indices [7]. Here the goal is to reduce the fuel cost and increase voltage profile simultaneously by reducing the voltage deviation of *PQ (load)* buses from the unity 1.0 *p.u.* Hence, the objective function may be formulated by following equation [5]:

$$Y = Y_{\cos t} + wY_{voltage-deviation} \tag{26}$$

Where, w is an appropriate weighting factor, to be chosen by the user to offer a weight or importance to each one of the two terms of the objective function. $Y_{\cos t}$ and $Y_{voltage-deviation}$ are specified as follows [5]:

$$Y_{\cos t} = \sum_{i=1}^{NLB} f_i \tag{27}$$

$$Y_{voltage\_deviation} = \sum_{i=1}^{NLB} |V_i - 1.0| \tag{28}$$

The variation of voltage deviation over iterations is sketched in Figure.3. It demonstrates that the suggested method has good convergence characteristics. The statistical values of voltage deviation obtained with different methods are shown in Table 3 which displays that the results obtained by MVO are better than the other methods. The optimal values of control variables obtained by MVO algorithm for case 2 are specified in Table 1. By means of the same settings, the results achieved in case 2 with the MVO technique are compared to some other methods and it displays that the voltage deviation is greatly reduced compared to the initial case [7]. It has been made known that the voltage deviation is reduced from 1.1496 *p.u.* to 0.1056 *p.u.* using MVO technique.

Table 1: Optimal values of control variables.

Control variable	**Min**	**Max**	**Case1**	**Case2**	**Case3**	**Case4**	**Case5**
P_{G1} (MW)	50	200	177.349	177.983	184,86	51.327	51.348
P_{G2} (MW)	20	80	48.712	48.765	50,563	80.000	80.000
P_{G5} (MW)	15	50	21.278	21.475	21,97	50.000	50.000
P_{G8} (MW)	10	35	20.962	20.158	10	35.000	35.000
P_{G11} (MW)	10	30	11.836	12.932	13,733	30.000	29.998
P_{G13} (MW)	12	40	12.000	12.029	12,1038	40.000	40.000
V_1(p.u)	0.95	1.1	1.100	1.045	1,099	1.100	1.100
V_2(p.u)	0.95	1.1	1.088	1.027	1,071	1.097	1.100
V_5(p.u)	0.95	1.1	1.061	1.010	1,028	1.081	1.093
V_8(p.u)	0.95	1.1	1.070	1.004	1,021	1.088	1.100
V_{11}(p.u)	0.95	1.1	1.100	1.065	1,094	1.100	1.100
V_{13}(p.u)	0.95	1.1	1.100	0.996	1,1	1.100	1.100
$T_{6\text{–}9}$	0	1.1	0.964	1.077	0,921	1.037	1.000
$T_{6\text{–}10}$	0	1.1	1.045	0.900	0,9458	0.901	0.937
$T_{4\text{–}12}$	0	1.1	1.038	0.928	0,938	0.994	0.993
$T_{28\text{–}27}$	0	1.1	0.990	0.965	0,925	0.987	0.983
$Qc_{10(}$Mvar)	0	5	3.525	4.973	5	0.306	0.775
Qc_{12}(Mvar)	0	5	1.770	0.716	5	3.082	3.857
Qc_{15}(Mvar)	0	5	2.029	0.382	5	4.552	3.668
Qc_{17}(Mvar)	0	5	2.028	0.434	5	0.815	2.923
Qc_{20}(Mvar)	0	5	3.514	3.092	4,997	2.787	4.170
Qc_{21}(Mvar)	0	5	2.415	4.398	5	1.106	2.113
Qc_{23}(Mvar)	0	5	1.551	5.000	5	4.987	3.390
Qc_{24}(Mvar)	0	5	2.997	3.000	5	2.308	5.000
Qc_{29}(Mvar)			3.991	2.234	5	3.825	2.952
Fuel cost ($/h)	**-**	**-**	**799.242**	803.908	802,466	967.143	967.250
Ploss (MW)	-	-	8.667	9.908	9,834	**2.881**	2.948
QLoss (MVAR)	-	-	-2.936	5.641	7,66466	-24.614	**-25.038**
Vd	-	-	1.591	**0.1056**	1,8607	1.975	2.041
Lmax	-	-	0.120	0.137	**0,11467**	0.118	0.117

Table 2: Comparison of fuel cost obtained with different algorithms.

Method	Fuel Cost	Method Description
MVO	**799.242**	Multi-verse Optimizer
FA	799.766	Firefly Algorithm
PSO	799.704	Particle Swarm Optimization
DE [6]	799.289	Differential Evolution
BHBO [7]	799.921	Black Hole Based Optimization

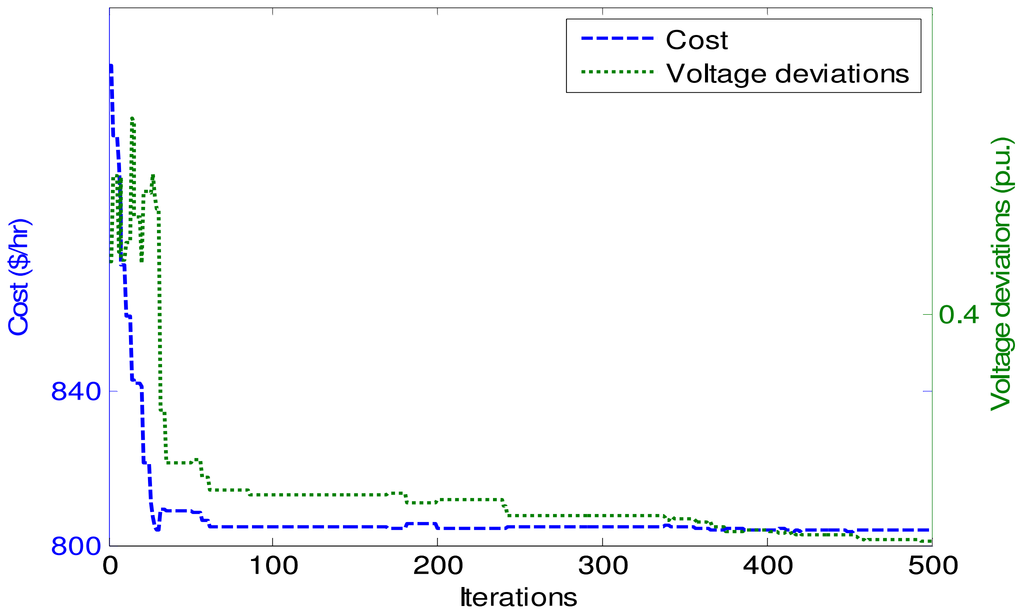

Figure.3 Variations of fuel cost and voltage deviations for Case 2.

Table 3: Comparison of voltage deviations obtained with different algorithms.

Method	Voltage Deviation	Method Description
MVO	**0.1056**	Multi-verse Optimizer
FA	0.1474	Firefly Algorithm
PSO	0.1506	Particle Swarm Optimization
DE	0.1357	Differential Evolution
BHBO [7]	0.1262	Black Hole Based Optimization

Case 3: Voltage stability enhancement

Presently, the transmission systems are enforced to work nearby their safety bounds, because of cost-effective and environmental causes. One of the significant characteristics of the system is its capability to retain continuously tolerable bus voltages to each node beneath standard operational environments, next to the rise in load, as soon as the system is being affected by disturbance. The unoptimized control variables may cause increasing and unmanageable voltage drop causing a tremendous voltage collapse [5]. Hence, voltage stability is inviting ever more attention. By using various techniques to evaluate the margin of voltage stability, Glitch and Kessel have introduced a voltage stability index called L-index depends on the viability of load flow equations for every node [25]. The L-index of a bus shows the probability of voltage collapse circumstance for that particular bus. It differs between 0 and 1 equivalent to zero load and voltage collapse, respectively.

For the given system with *NB, NGen* and *NLB* buses signifying the total no. of buses, the total no. of generator buses and the total no. of load buses, respectively. The buses can be distinct as *PV (generator)* buses at the head and *PQ (load)* buses at the tail as follows [5]:

$$\begin{bmatrix} I_L \\ I_G \end{bmatrix} = [Y_{bus}] \begin{bmatrix} V_L \\ V_G \end{bmatrix} = \begin{bmatrix} Y_{LL} & Y_{LG} \\ Y_{GL} & Y_{GG} \end{bmatrix} \begin{bmatrix} V_L \\ V_G \end{bmatrix} \tag{29}$$

Where, Y_{LL}, Y_{LG}, Y_{GL} and Y_{GG} are co-matrix of Y_{bus}. The subsequent hybrid system of equations can be expressed as:

$$\begin{bmatrix} V_L \\ I_G \end{bmatrix} = [H] \begin{bmatrix} I_L \\ V_G \end{bmatrix} = \begin{bmatrix} H_{LL} & H_{LG} \\ H_{GL} & H_{GG} \end{bmatrix} \begin{bmatrix} I_L \\ V_G \end{bmatrix} \tag{30}$$

Where matrix *H* is produced by the partially inversing of Y_{bus}, H_{LL}, H_{LG}, H_{GL} and H_{GG} are co- matrix of *H*, V_G, I_G, V_L and I_L are voltage and current vector of Generator buses and load buses, respectively.

The matrix *H* is given by:

$$[H] = \begin{bmatrix} Z_{LL} & -Z_{LL}Y_{LG} \\ Y_{GL}Z_{LL} & Y_{GG} - Y_{GL}Z_{LL}Y_{LG} \end{bmatrix} Z_{LL} = Y_{LL}^{-1} \tag{31}$$

Hence, the L-index denoted by L_j of bus j is represented as follows:

$$L_j = \left| 1 - \sum_{i=1}^{NLB} H_{LG_{ji}} \frac{v_i}{v_j} \right| \quad j=1,2\ldots,NL \tag{32}$$

Hence, the stability of the whole system is described by a global indicator $L_{\max}$ which is given by [7],

$$L_{\max} = \max(L_j) \qquad j=1,2\ldots,NL \tag{33}$$

The system is more stable as the value of $L_{\max}$ is lower.

The voltage stability can be enhanced by reducing the value of voltage stability indicator *L-index* at every bus of the system. [7].

Thus, the objective function may be given as follows:

$$Y = Y_{\cos t} + wY_{voltage\_Stability\_Enhancement} \tag{34}$$

$$\text{Where, } Y_{\cos t} = \sum_{i=1}^{NLB} f_i \tag{35}$$

$$Y_{voltage\_stability\_enhancement} = L_{\max} \tag{36}$$

The variation of the *Lmax* index over iterations is presented in Figure. 4. The results obtained with different methods are shown in Table 4 which displays that MVO method gives better results than the other methods. The optimal values of control variables obtained by MVO algorithm for case 3 are given in Table 1. After applying the MVO technique, it appears from Table 1 that the value of *Lmax* is considerably decreased in this case compared to initial case [7] from 0.1723 to 0,11467. Thus, the distance from breakdown point is improved.

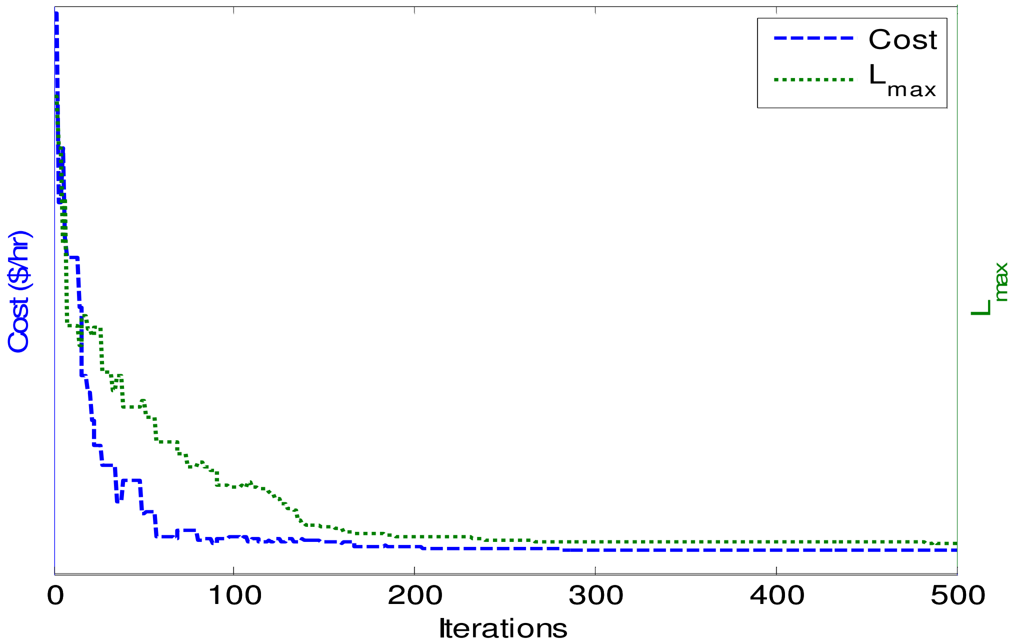

Figure.4 Variations of fuel cost and stability index for Case 3.

Table 4: Comparison of *Lmax* index obtained with different algorithms.

Method	L_{max}	Method Description
MVO	**0,11467**	Multi-verse Optimizer
FA	0.1184	Firefly Algorithm
PSO	0.1180	Particle Swarm Optimization
DE [6]	0.1219	Differential Evolution
BHBO [7]	0.1167	Black Hole Based Optimization

Case 4: Minimization of active power transmission losses

In the case 4 the Optimal Power Flow objective is to reduce the active power transmission losses, which can be represented by power balance equation as follows [7]:

$$J = \sum_{i=1}^{NLB} P_i = \sum_{i=1}^{NLB} P_{Gi} - \sum_{i=1}^{NLB} P_{Di} \tag{37}$$

Figure.5 shows the tendency for reducing the total real power losses objective function using the MVO algorithm. The active power losses obtained with different techniques are shown in Table 5 which made sense that the results obtained by MVO give better values than the other methods. The optimal values of control variables obtained by the proposed algorithm for case 4 are displayed in Table 1. By means of the same settings the results achieved in case 4 with the MVO technique are compared to some other methods and it displays that the real power transmission losses are greatly reduced compared to the initial case [7] from 5.821 MW to 2.881 MW.

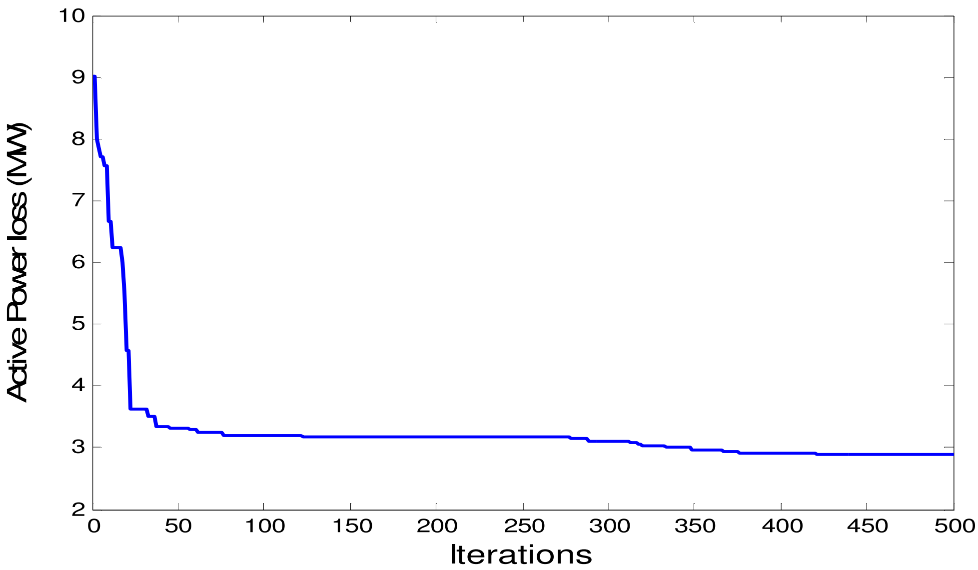

Figure.5 Variations of active power transmission losses for Case 4.

Table 5: Comparison of active power transmission losses obtained with different algorithms.

Method	Active Power Loss	Method Description
MVO	**2.881**	Multi-verse Optimizer
FA	3.307	Firefly Algorithm
PSO	3.026	Particle Swarm Optimization
BHBO [7]	3.503	Black Hole Based Optimization

Case 5: Minimization of reactive power transmission losses

The accessibility of reactive power is the main point for static system voltage stability margin to support the transmission of active power from the source to sinks [7].
Thus, the minimization of *VAR* losses are given by the following expression:

$$J = \sum_{i=1}^{NLB} Q_i = \sum_{i=1}^{NLB} Q_{Gi} - \sum_{i=1}^{NLB} Q_{Di} \tag{38}$$

It is notable that the reactive power losses are not essentially positive. The variation of reactive power losses shown in Figure.6. It demonstrates that the suggested method has good convergence characteristics. The values of reactive power losses obtained with different methods are shown in Table 6, which displays that the results obtained by MVO are better than the other methods. The optimal values of control variables obtained by the proposed algorithm for case 5 are given in Table 1. It is shown that the reactive power losses are greatly reduced compared to the initial case [7] from -4.6066 to -25.038 using MVO technique.

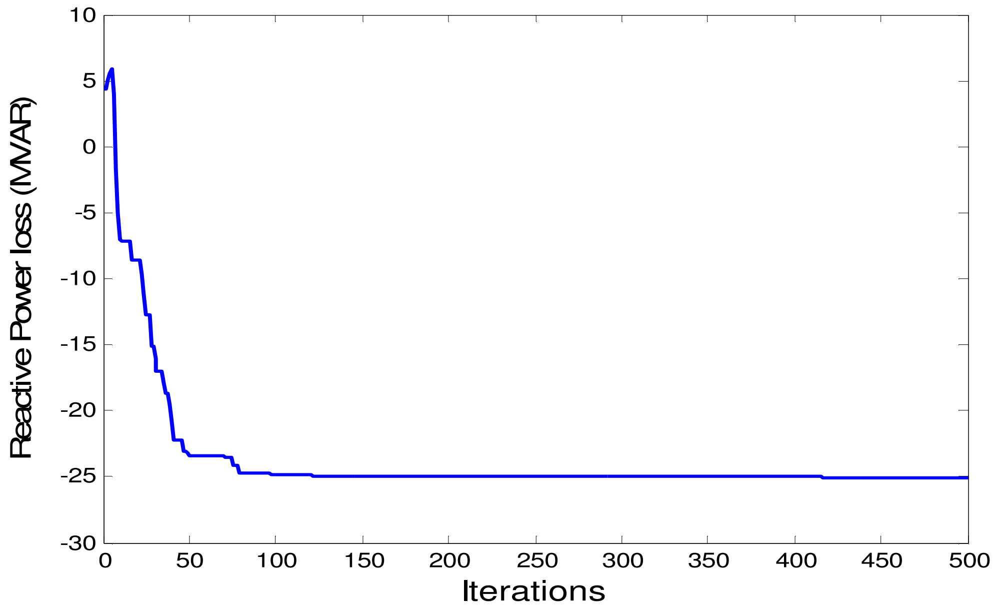

Figure.6 Variations of reactive power transmission losses for Case 5.

Table 6 Comparison of reactive power losses obtained with different algorithms.

Method	Reactive Power Loss	Method Description
MVO	**-25.038**	Multi-verse Optimizer
FA	-20.464	Firefly Algorithm
PSO	-23.407	Particle Swarm Optimization
BHBO [7]	-20.152	Black Hole Based Optimization

4.2 IEEE 57-bus system

To prove the substance and robustness of the proposed approach in solving OPF problem in large power system, the IEEE 57-bus with 80 branch systems has been proposed in this party, which has a 34 control variables as follows: 7 generator voltage magnitudes, 17 transformer-tap settings, and 3 bus shunt reactive compensators. The maximum voltage magnitude of all bus is 1.1 p.u and the minimum voltage magnitude is 0.95. The total system demand is 12.508 p.u. for the active power, and 3.364 p.u for the reactive power at 100 MVA base, bus 1 is taken as slack bus. The values of coefficients fuel costs of the seven generators are presented in [14]**.** Figure.7 shows that the MVO algorithm has converged to the global optimal solution after 200 iterations. It is obvious that MVO increases the convergence speed which obtains better final results. The proposed methods give us the results shown in Table 7. We compared with other method in literature in Table 8. The best fuel cost obtained by the proposed MVO is 41678.0847 $/h, that is better than reported in [21-24]. This comparison shows the effectiveness and the robustness of the proposed algorithm.

Table 7. Optimal settings of control variables for IEEE 57-bus system.

Control variable (p.u.)	MVO
P1 (p.u)	142,0727988
P2 (p.u)	85,29053212
P3 (p.u)	44,10864
P6 (p.u)	72,56587168
P8 (p.u)	461,5017056
P9 (p.u)	100
P13 (p.u)	360,4355589
V1 (p.u)	1,038860619
V2 (p.u)	1,043946394
V3 (p.u)	1,0330335
V6 (p.u)	1,051732939
V8 (p.u)	1,065709946
V9 (p.u)	1,040972354
V13 (p.u)	1,022939856
T4-18	0,970174762
T4-18	0,9
T21-20	0,903747067
T24–25	1,1
T24–25	1,003408012
T24–26	1,08574421
T7–29	0,951256711
T34–32	1,046256308
T11–41	0,971718857
T15–45	1,086471491
T14–46	0,994206114
T10–51	1,075111678
T13–49	1,1
T11–43	0,983198039
T40–56	1,1
T39–57	1,1
T9–55	1,1
QC18 (MVAr)	10,16384811
QC25 (MVAr)	12,00183602
QC53 (MVAr)	11,11143839
Fuel cost ($/h)	**41678.0847**
Ploss (MW)	15.1751

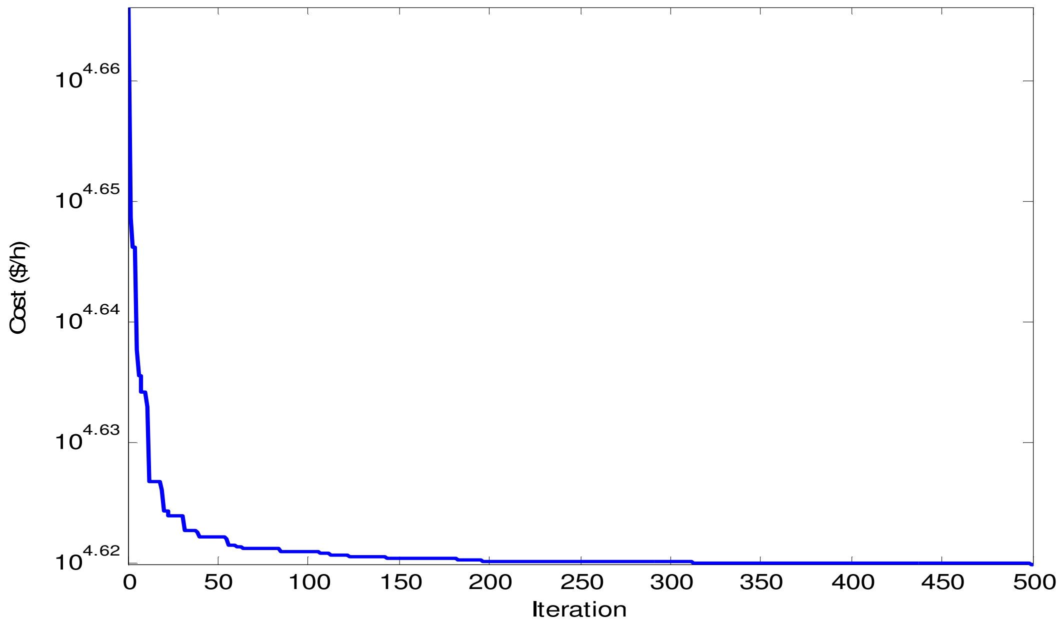

Figure.7. Fuel cost variation for IEEE 57-bus system..

Table 8.Comparison of results for a IEEE 57-bus system.

Algorithms	Fuel cost ($/h)
MVO	41678.0847
TLBO[21]	41695.6626
LDI-PSO[22]	41815.5035
GSA[23]	41695.8717
ABC[22]	41693.9589
EADDE[24]	41713.62

Statistically: According to the all results obtained through the minimization of treated objectives, I wish to note that the process has run 50 times with different initial solutions for case 1, Table 9 indicates that algorithm offers the minimum values of best, worst, median values of fuel cost, and the average of the average total computational times. we can show that time of proposed MVO method is low, as well as note the difference between the minimum and the worst is very close, this is also shown by the low values of the standard deviations calculated from it we can say that the proposed method is robust.

Table 9. Statistical results for case 1.

Methods	Best	Median	Worst	STD	Avr CPU time (s)
MVO	**799.2420**	799.3776	799.7820	0.1833	24.87

5. Conclusion

In this study, Multi-verse Optimizer has been presented and applied to solving the OPF problem. The program can treat different objectives in order to: Minimization of generation fuel cost, voltage profile improvement, voltage stability enhancement , minimization of active power transmission losses, minimization of reactive power transmission losses. Through the applications that made on the IEEE 30-bus and IEEE 57-bus test systems, the solutions obtained from the MVO approach has good convergence characteristics and gives the better results compared to FA and PSO methods and other method reported in litterateur which confirm the effectiveness of proposed algorithm.

6. References

[1] H.R.E.H. Bouchekara, M.A. Abido, A.E. Chaib, R. Mehasni, Optimal power flow using the league championship algorithm: a case study of the Algerian power system, Energy Convers. Manag. 87 58–70,2014.

[2] Duman S, Güvenç U, Sönmez Y, Yörükeren N. Optimal power flow using gravitational search algorithm. Energy Convers Manag;59:86–95,2012.

[3] Niknam T, R Narimani M, Jabbari M, Malekpour AR. A modified shuffle frog leaping algorithm for multi-objective optimal power flow. Energy 2011;36(11):6420–32

[4] J. Carpentier, Contribution à l'étude du Dispatching Economique, Bull. Soc. Fran-caise Electriciens 431–447,1962.

[5] H.R.E.H. Bouchekara, M.A. Abido, M. Boucherma, Optimal power flow using Teaching-Learning-Based Optimization technique, Electr. Power Syst. Res. 114;49–59,2014.

[6] A.A. Abou El Ela, M.A. Abido, Optimal power flow using differential evolution algorithm, Electr. Power Syst. Res. 80 (7) 878–885,2010.

[7] Bouchekara, H. R. E. H. Optimal power flow using black-hole-based optimization approach. Appl. Soft Comput. **24,** 879–888 2014.

[8] S. Frank, I. Steponavice, S. Rebennack, Optimal power flow: a bibliographic survey I, formulations and deterministic methods, Energy Syst. 3 (3) 221–258,2012.

[9] M.R. AlRashidi, M.E. El-Hawary, Applications of computational intelligence techniques for solving the revived optimal power flow problem, Electr. PowerSyst. Res. 79 (4)694–702,2009.

[10] S. Frank, I. Steponavice, S. Rebennack, Optimal power flow: a bibliographic survey II, non-deterministic and hybrid methods, Energy Syst. 3 (3) 259–289,2012.

[11] A.R. Yildiz, A comparative study of population-based optimization algorithms for turning operations, Inf. Sci. (Ny) 210 81–88,2012.

[12] Ouafa Herbadji , Linda Slimani and Tarek Bouktir. Solving Bi-Objective Optimal Power Flow using Hybrid method of Biogeography-Based Optimization and Differential Evolution Algorithm: A case study of the Algerian Electrical Network J. Electrical Systems 12-1:197-215,2016.

[13] Bachir Bentouati. Lakhdar Chaib and Saliha Chettih. Optimal Power Flow using the Moth Flam Optimizer: A case study of the Algerian power system, Indonesian Journal of Electrical Engineering and Computer Science.;1:3,2016.

[14] K. Lee, Y. Park, J. Ortiz, A united approach to optimal real and reactive power dispatch, IEEE Trans. Power App. Syst. 104 (5) 1147–1153,1985.

[15] Mirjalili, S., Mohammad, S. & Hatamlou, A. Multi-Verse Optimizer: a nature-inspired algorithm for global optimization. doi:10.1007/s00521-015-1870-7,2015.

[16] A.G. Bakirtzis, P.N. Biskas, C.E. Zoumas, V. Petridis, Optimal power flow by enhanced genetic algorithm, IEEE Trans. Power Syst. 17 (2) 229–236,2002.

[17] W. Ongsakul, T. Tantimaporn, Optimal power flow by improved evolutionary programming, Electr. Power Compon. Syst. 34 (1) 79–95,2006.

[18] C.A. Belhadj, M.A. Abido, An optimized fast voltage stability indicator, in: Electric Power International Conference on Engineering, PowerTech Budapest, pp. 79–83, 1999.

[19] S.A.H. Soliman, A.H. Mantawy, Modern Optimization Techniques with Applications in Electric Power Systems, Energy Systems, Springer, New York/Heidelberg/Dordrecht/London, 2012.

[20] T. Bouktir, R. Labdani, L. Slimani, Optimal power flow of the Algerian electrical network using ant colony optimization method, Leoanardo J. Sci.43–57,2005.

[21] M. Ghasemi, S. Ghavidel, M. Gitizadeh, and E. Akbari, "An improved teaching-learning-based optimization algorithm using Levy mutation strategy for non-smooth optimal power flow," Int. J. Electr. Power Energy Syst., vol. 65, no. C, pp. 375–384, 2015.

[22] M. Rezaei Adaryani and a. Karami, "Artificial bee colony algorithm for solving multi-objective optimal power flow problem," Int. J. Electr. Power Energy Syst., vol. 53, pp. 219–230, 2013.

[23] S Duman U Güvenç. Y Sönmez. and N Yörükeren. Optimal power flow using gravitational search algorithm.Energy Convers, Manag.59:86–95,2012.

[24] K. Vaisakh and L. R. Srinivas, "Evolving ant direction differential evolution for OPF with non-smooth cost functions," *Eng. Appl. Artif. Intell.*, vol. 24, no. 3, pp. 426–436, 2011.

[25] P. Kessel, H. Glavitsch, Estimating the voltage stability of a power system, IEEETrans. Power Deliv. 1 (3) 346–354,1986.